Discrete Dynamics in Nature and Society, Vol. 5, pp. 107–120
Reprints available directly from the publisher
Photocopying permitted by license only

© 2000 OPA (Overseas Publishers Association) N.V.
Published by license under
the Gordon and Breach Science
Publishers imprint.
Printed in Malaysia.

Staircase Baker's Map Generates Flaring-type Time Series

G. C. HARTMANN*, G. RADONS, H. H. DIEBNER and O. E. ROSSLER

Division of Theoretical Chemistry, Auf der Morgenstelle 8, University of Tübingen, 72076 Tübingen, FRG

(Received 27 December 1999)

The baker's map, invented by Eberhard Hopf in 1937, is an intuitively accesible, two-dimensional chaos-generating discrete dynamical system. This map, which describes the transformation of an idealized two-dimensional dough by stretching, cutting and piling, is non-dissipative. Nevertheless the "x" variable is identical with the dissipative, one-dimensional Bernoulli-shift-generating map. The generalization proposed here takes up ideas of Yaacov Sinai in a modified form. It has a staircase-like shape, with every next step half as high as the preceding one. Each pair of neighboring elements exchanges an equal volume (area) during every iteration step in a scaled manner. Since the density of iterated points is constant, the thin tail (to the right, say) is visited only exponentially rarely. This observation already explains the map's main qualitative behavior: The "x" variable shows "flares". The time series of this variable is closely analogous to that of a flaring-type dissipative dynamical system – like those recently described in an abstract economic model. An initial point starting its journey in the tale (or "antenna", if we tilt the map upwards by 90 degrees) is predictably attracted by the broad left hand (bottom) part, in order to only very rarely venture out again to the tip. Yet whenever it does so, it thereby creates, with the top of a flare, a new "far-from-equilibrium" initial condition, in this reversible system. The system therefore qualifies as a discrete analogue to a far-from-equilibrium multiparticle Hamiltonian system. The height of the flare hereby corresponds to the momentary height of the H function of a gas. An observable which is even more closely related to the momentary negative entropy was recently described. Dependent on the numerical accuracy chosen, "Poincaré cycles" of two different types (periodic and nonperiodic) can be observed for the first time.

Keywords: Flare attractors; Baker's map; Multi-baker's map; Poincaré cycles; Boltzmann H function

1. INTRODUCTION

Can reversible systems flare? To show that the answer is yes, it makes sense to first briefly recall what flaring-type behavior is like in *dissipative* dynamical systems. Everybody knows what a sun flare is; also, economic systems can flare – when they show the typical rise and downfall of an

*Corresponding author.

entrepreneurial empire, for example [1–3]. A flare in a dynamical system is characterized by a finite time of autocatalytic growth, with a (during that period) momentarily positive "Lyapunov-characteristic exponent" (LCE), even though the same variable asymptotically speaken is damped (has a negative LCE) [4]. Flaring-type attractors are generalized Milnor [5] attractors. Milnor attractors possess "riddled basins" in which arbitrarily close initial conditions end up, with a finite probablity, at a different attractor. While Milnor attractors are structurally unstable, flare attractors are generic and indeed prototypal. Flare attractors arise, for example, in neural networks, as recent work by Tsuda and Nicolis [6] suggests. They are also useful in automatic pattern classification [4].

The time series shown in Figure 1 has been generated by the perhaps simplest example of a flare attractor, described by:

$$x_{n+1} = 2x_n \mod 1 = 2x_n + \begin{cases} 0 & \text{if } x_n \le \frac{1}{2} \\ -1 & \text{if } x_n > \frac{1}{2} \end{cases}$$

$$y_{n+1} = y_n + (x_n - 0.67)y_n + 10^{-2} - 10^{-3}y_n^2 \qquad (1)$$

The system of Eq. (1) is a typical dissipative, noninvertible nonlinear dynamical systems, written in the form of a noninvertible 2D map. While the first variable generates the random time behavior of the Bernouilli-shift ("chaos"), the second variable is either negatively or positively

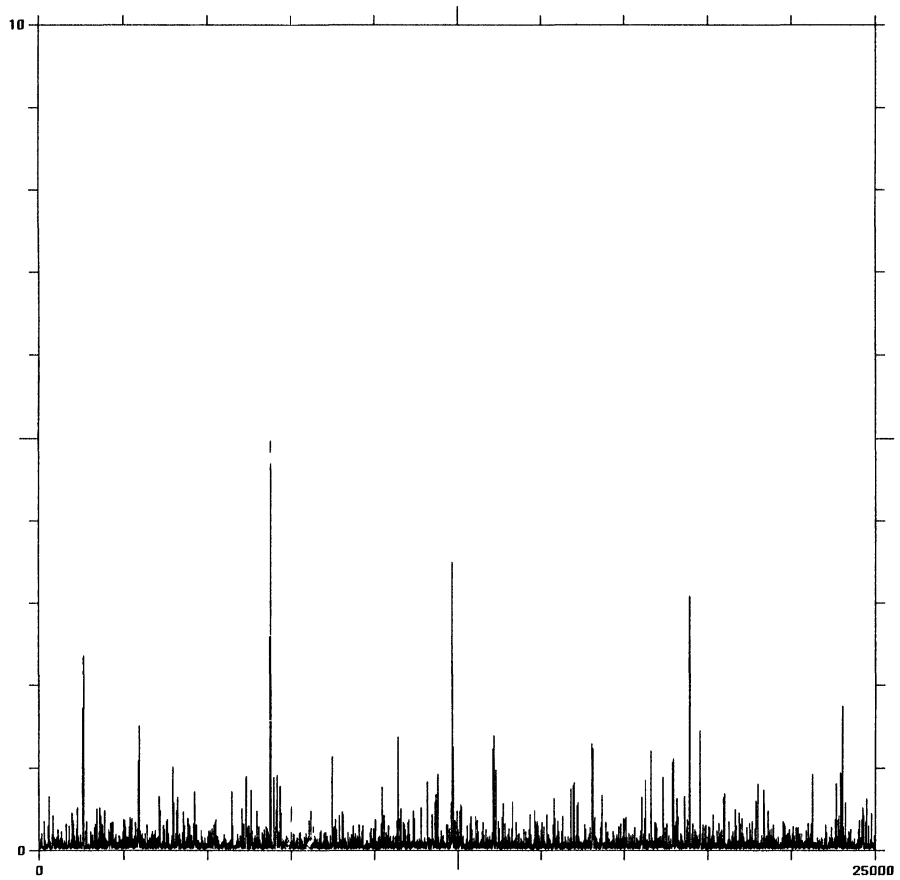


FIGURE 1 Times series of a flare attractor. Numerical simulation of the Bernouilli-shift based flare attractor equation, Eq. (1), second variable. 25 000 iterations are shown. Initial conditions: $x_0 = 0.1 \cdot \sqrt{2}$, $y_0 = 0.1$.

damped, depending on the momentary value of x. This is the secret of "flaring" [3].

If one wants to have the same behavior in a continuous invertible dynamical system, one needs four variables at least instead of two [4]. Three alone are needed for the chaos generator (which in the case of Eq. (1) has been reduced to a non-invertible 1D map, the Bernouilli-shift generator). The fourth variable – in Eq. (1), the second variable – is in the simplest case passively forced by the signal coming from the forcing chaotic subsystem. This is also the case with the second variable in Eq. (1). Virtually the same right-hand side can be used in a continuous system [4].

The conditions for flaring are somewhat critical: The passively forced y-variable has to be lifted beyond a threshold value of (zero) negative damping, before autonomous autocatalytic growth (elicited by "supra-threshold" values of the chaotic input) can set in. In Eq. (1), the threshold value of x used is 0.67. Evidently, every gap-less chaotic input contains, with a certain probability, subsequences of symbols (supra-threshold amplitudes of x) of any length leading to sustained autocatalytic growth over that length of time. The latter sequences then generate a flare of matching duration each. The latter is accompanied by an exponentially increasing (with the duration of the supra-threshold input sequence) height. While this behavior is robust, it is a somewhat non-trivial task numerically to adjust the threshold in the responding variable (the subtracted constant inside the bracket in the second line of Eq. (1) in such a way that a "beautiful" sequence of flares results.

2. FLARING IN REVERSIBLE SYSTEMS

In an early paper, Carl-Friedrich von Weizsäcker [7] exposed the essence of the scandal of far-from-equilibrium behavior in reversible dynamical systems as it had been introduced by Ludwig Boltzmann (*cf.* [8]). He convincingly showed that, whenever such a system finds itself in a far-from-equilibrium state, the probability that it was yesterday in an even more far-away state is negligible compared to the assumption that it momentarily peaks in its present (less far-away) initial condition. In consequence, if we wake up in the morning and believe that yesterday existed, the probability of our only believing this on the basis of our momentary, far-from-equilibrium brain state is much greater than that we indeed got enough food to eat yesterday to reach that brain state legitimately from an even more improbable initial condition the day before.

Hence Boltzmann's idea of reversible systems reaching far-from-equilibrium conditions spontaneously (if very rarely) in an almost infinite available period of time, in order to from there straightforwardly proceed to closer-to-equilibrium states again, indeed borders on believing in a miracle. In the following, an explicit equation which illustrates this "miracle" allows one to inspect and scrutinize it will be presented – in the form a discrete reversible system with flaring-type behaviour.

3. THE STAIRCASE BAKER'S MAP

The basic staircase map is shown in Figure 2. The four-step version shown in the figure can be elongated up to an arbitrary number of steps by intercalating further middle elements (like the second or the third). The principle behind the design of the staircase baker's map can be understood by one's having a look at the multiple baker's map of Figure 3, which was in similar form first indicated by Hopf [9], in §17 of his chapter four. The original baker's map, in turn, which is still simpler, is shown in Figure 4.

The original baker's map (to start out from the simplest case) was invented by Eberhard Hopf in 1937 [9]. A piece of dough is elongated by means of the rolling-pin operator, to become half as high and twice as long as before. Then, the knife operator is used to cut the dough in two equal-length halves, of which the right-hand portion is then piled on (put on top of) the left-hand one.

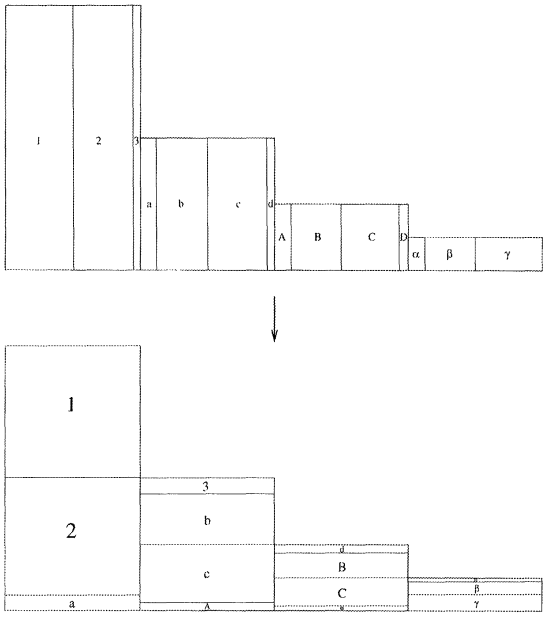


FIGURE 2 Staircase map.

The procedure is iterated. While Hopf [9] did not mention the details of the two operators, he made the revealing remark that this is how fluffy pastry is made in a bakery. The name "baker's transformation" was given to the map by John von Neumann in a talk at Princeton in 1949 (Eberhard Hopf, personal communication 1977).

The baker's map is a "mixing transformation" [9]. It preserves phase-space volume and is ergodic. The horizontal variable (x) doubles length at every step in a "modulo" fashion; its behavior is described by the Bernoulli-shift generator, already put to good use in the first line of Eq. (1) above. The vertical second variable (y) halves the height of the dough with every step. The full equation of the baker's transformation thus reads:

$$\begin{aligned} x_{n+1} &= 2x_n \bmod 1 \\ y_{n+1} &= \frac{1}{2}y_n + \begin{cases} 0 & \text{if } x_n \leq \frac{1}{2} \\ \frac{1}{2} & \text{if } x_n > \frac{1}{2} \end{cases} \end{aligned} \tag{2}$$

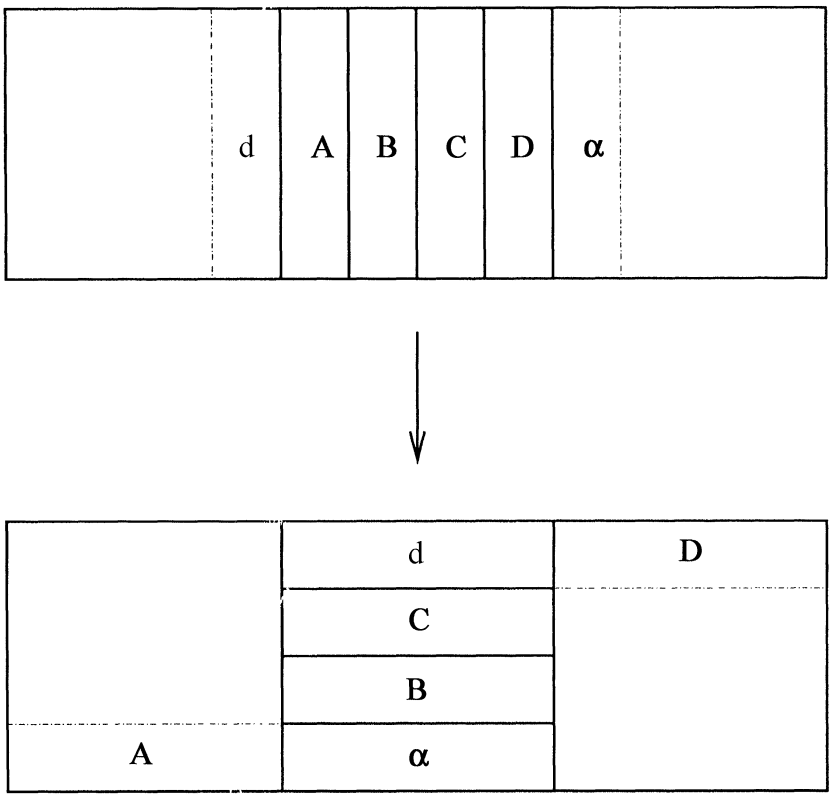


FIGURE 3 A Hopf-like map (*cf.* text).

While this description is the most convenient one to use, we note in passing that Hopf's own algebraic description of his map looked rather different [9].

To understand the map of Figure 2, we work our way backwards starting from Figure 4. Note that in Figure 4, the left-hand volume (area $A + B$), interpreted as "dough", is first "rolled out" (with a rolling pin) to reach half its former height and twice its former length, and then "cut" in the middle (with a knife) so that the right-hand half portion (B) comes to lie on the top of the left-hand portion (A); then the whole procedure is repeated [10]. Next, we come to the four-piece map of Figure 3. If pieces A and D occupied the places of α and d, in the middle portion of the first iterate of the map (lower part of Fig. 3), a four-piece version of the original Hopf baker's map of Figure 4 would pertain. Thus, the full multi-baker's map is nothing else but an ordinary four-piece baker's map put beside ifself arbitrarily many times – yet with each pair of neighboring elements exchanging an equal-size piece of "dough" at every step.

We now equipped to proceed to the explicit description of the staircase baker's map of Figure 2 itself. The only difference to the "Hopf-like" map of Figure 3 is the reduction in height by a constant factor, from each submap to the next. One sees that the width of a rightmost element (for example, D in Fig. 2) and the width of a leftmost element (for example, α) differ by a constant factor (two in the figure), to allow for equal volumes (areas) of the two exchanged pieces. In consequence, again an equal amount of "dough" is exchanged between neighboring elements per iteration step – just as this was the case in the constant-height map of Figure 3.

The following explicit equation can be used for the map of Figure 2 with n steps:

$$
x_{n+1} = \begin{cases}
\quad [\text{if } 0 < x_n \le 1 :] & \\
\frac{100}{50}\, x_n & \text{if } 0 < x_n \le \frac{50}{100} \\
\frac{100}{44}\left(x_n - \frac{50}{100}\right) & \text{if } \frac{50}{100} < x_n \le \frac{94}{100} \\
\frac{100}{6}\left(x_n - \frac{94}{100}\right) + 1 & \text{if } \frac{94}{100} < x_n \le 1 \\
\quad [\text{if } 1 < x_n \le m :] & \\
\frac{100}{12}\left(x_n - k_n\right) + k_n - 1 & \text{if } k_n < x_n \le \left(k_n + \frac{12}{100}\right) \\
\frac{100}{38}\left(x_n - \left(k_n + \frac{12}{100}\right)\right) + k_n & \text{if } \left(k_n + \frac{12}{100}\right) < x_n \le \left(k_n + \frac{50}{100}\right) \\
\frac{100}{44}\left(x_n - \left(k_n + \frac{50}{100}\right)\right) + k_n & \text{if } \left(k_n + \frac{50}{100}\right) < x_n \le \left(k_n + \frac{94}{100}\right) \\
\frac{100}{6}\left(x_n - \left(k_n + \frac{94}{100}\right)\right) + k_n + 1 & \text{if } \left(k_n + \frac{94}{100}\right) < x_n \le (k_n + 1) \\
\quad [\text{if } m < x_n \le (m+1) :] & \\
\frac{100}{12}\left(x_n - m\right) + m - 1 & \text{if } m < x_n \le \left(m + \frac{12}{100}\right) \\
\frac{100}{38}\left(x_n - \left(m + \frac{12}{100}\right)\right) + m & \text{if } \left(m + \frac{12}{100}\right) < x_n \le \left(m + \frac{50}{100}\right) \\
\frac{100}{50}\left(x_n - \left(m + \frac{50}{100}\right)\right) + m & \text{if } \left(m + \frac{50}{100}\right) < x_n \le (m+1)
\end{cases}
$$

$$y_{n+1} = \begin{cases} \frac{50}{100} y_n + \frac{50}{100} & \text{if } 0 < x_n \leq \frac{50}{100} \\ \frac{44}{100} y_n + \frac{6}{100} & \text{if } \frac{50}{100} < x_n \leq \frac{94}{100} \\ \frac{6}{100} y_n + \frac{44}{100} & \text{if } \frac{94}{100} < x_n \leq 1 \\ \frac{12}{100} y_n + \frac{88}{100} \cdot \frac{1}{2^{k_n}} - \frac{88}{100} \cdot \frac{1}{2^{k_n}} & \text{if } k_n < x_n \leq \left(k_n + \frac{12}{100}\right) \\ \frac{38}{100} y_n + \frac{50}{100} \cdot \frac{1}{2^{k_n}} & \text{if } \left(k_n + \frac{12}{100}\right) < x_n \leq \left(k_n + \frac{50}{100}\right) \\ \frac{44}{100} y_n + \frac{6}{100} \cdot \frac{1}{2^{k_n}} & \text{if } \left(k_n + \frac{50}{100}\right) < x_n \leq \left(k_n + \frac{94}{100}\right) \\ \frac{6}{100} y_n + \frac{88}{100} \cdot \frac{1}{2^{k_n+1}} & \text{if } \left(k_n + \frac{94}{100}\right) < x_n \leq (k_n + 1) \\ \frac{12}{100} y_n + \frac{88}{100} \cdot \frac{1}{2^m} - \frac{88}{100} \cdot \frac{1}{2^m} & \text{if } m < x_n \leq \left(m + \frac{12}{100}\right) \\ \frac{38}{100} y_n + \frac{50}{100} \cdot \frac{1}{2^m} & \text{if } \left(m + \frac{12}{100}\right) < x_n \leq \left(m + \frac{50}{100}\right) \\ \frac{50}{100} y_n & \text{if } \left(m + \frac{50}{100}\right) < x_n \leq (m + 1) \end{cases} \tag{3}$$

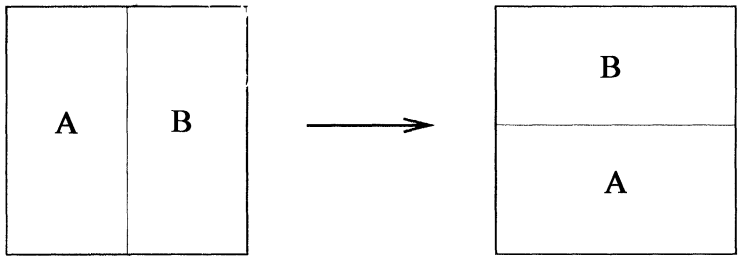


FIGURE 4 The baker's map of Eberhard Hopf.

Hereby the convention $k_n = \text{trunc}(x_n) = x_n - (x_n - \text{mod}1)$ has been used, which keeps track of the momentarily valid (visited) box at the nth time step. A numerical simulation of Eq. (3) is presented in Figure 5.

Equation (3) can be transformed into a numerical code that is exact, up to a given arbitrary finite number of digits, by means of the GNU Multiple Precision Library (GMP) using the *C* programming language, for example. As a sample, we show here the transformation that has to be applied to the straightforward *C* programming code of an explicit short part of Eq. (3), quoted explicitly in the upper part.:

- original *C*-code:

```
if (x < = 0.50) {
        x = 2.0 * x;
        y = 0.5 * y + 0.5;
}
```

- *C*-code using the GMP-library:

```
if(mpf_cmp(xx, o5) < = 0) {
  mpf_mul(xx, two0, xx);
  mpf_mul(du, o5, yy);
  mpf_add(yy, du, o5);
}
```

(4)

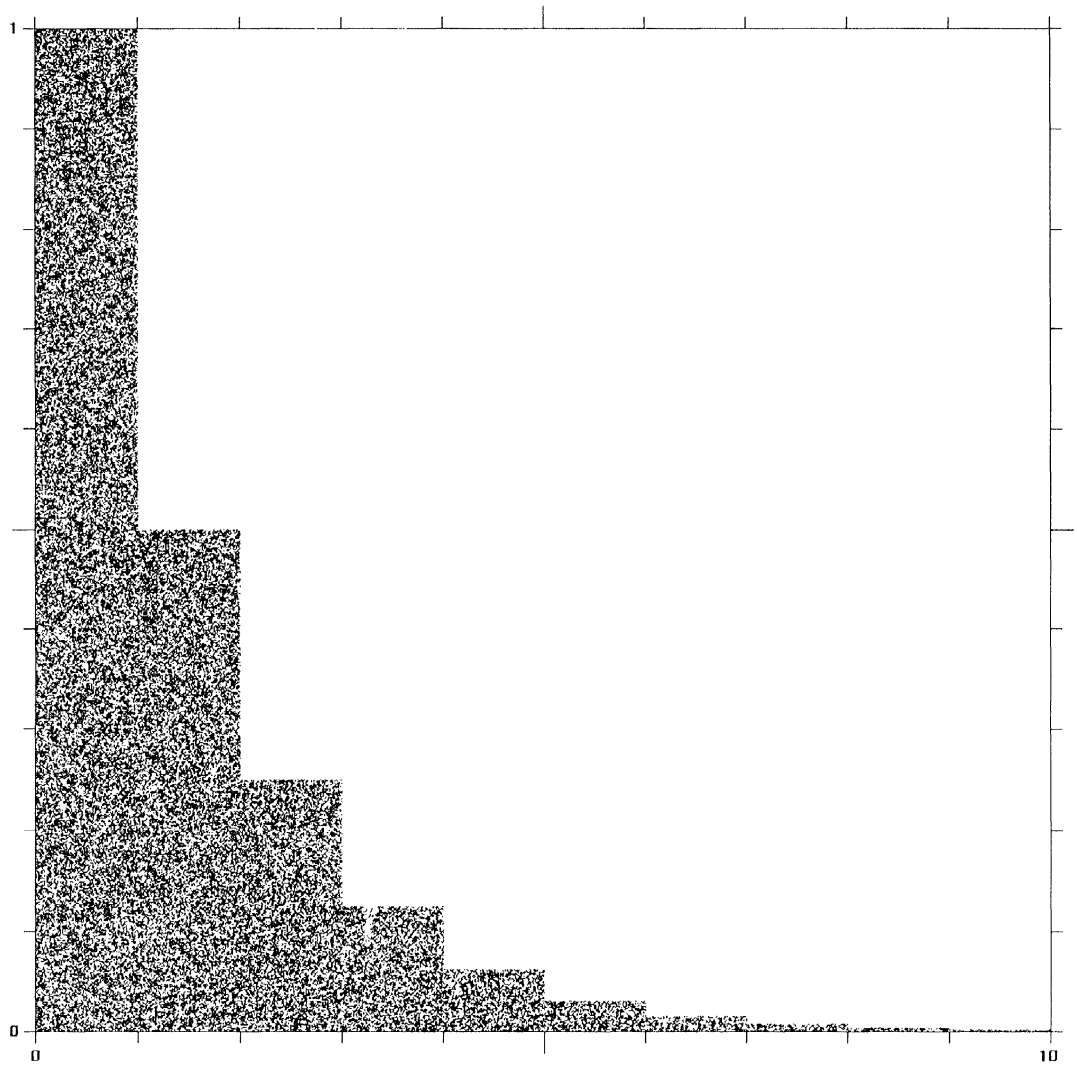


FIGURE 5 Staircase baker's map, with the vertical height blown up tenfold. Numerical simulation of Eq. (3) using a 16-decimal-digits accuracy ("double precision"). 100 000 iterations; $m = 40$. Only 10 stairs are shown.

One sees that the names of the variables were chosen in such a way as to be easily memorizable.

4. NUMERICAL PICTURES: THE TOWER OF BABEL

Figure 5 above already showed a fourty-piece version of the map of Figure 2 as described by Eq. (3). With a resolution of the plot of about 100 000 pixels per abscissa, an almost totally gray "staircase-in-concrete" resulted.

We now turn the picture around of Figure 5 by 90 degrees so that the right-hand "tail" becomes a vertical "antenna". We also augment it by a second copy on the right that has been flipped around for convenience of inspection to obtain Figure 6. The two half pictures, combined, give the impression of a tower with a very thin vertical needle in the middle as its crowning tip (or

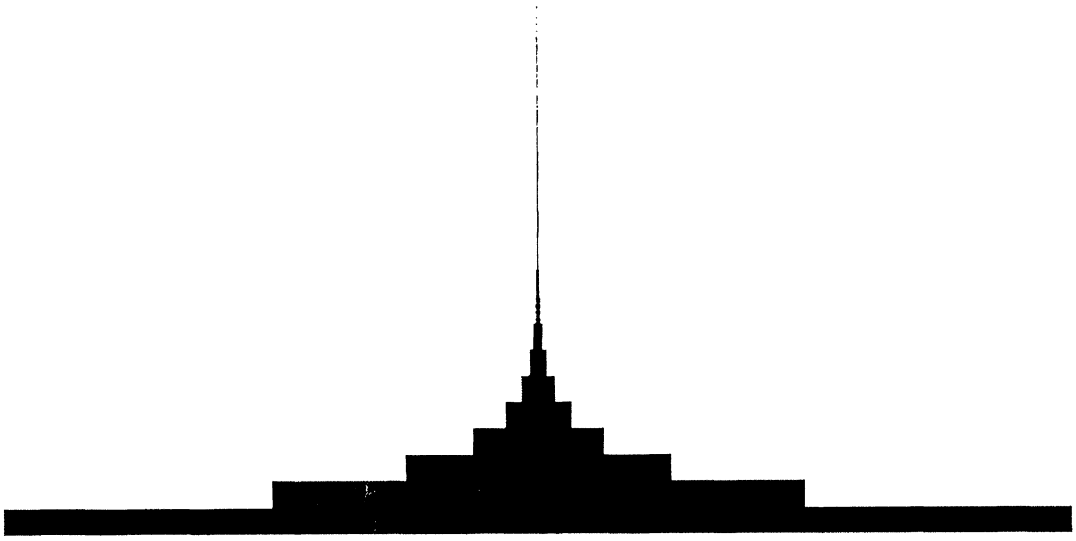


FIGURE 6 "Tower of Babel" (a turnedup- plus -mirrored version of Fig. 5). 500 000 iterations. *Cf.* text.

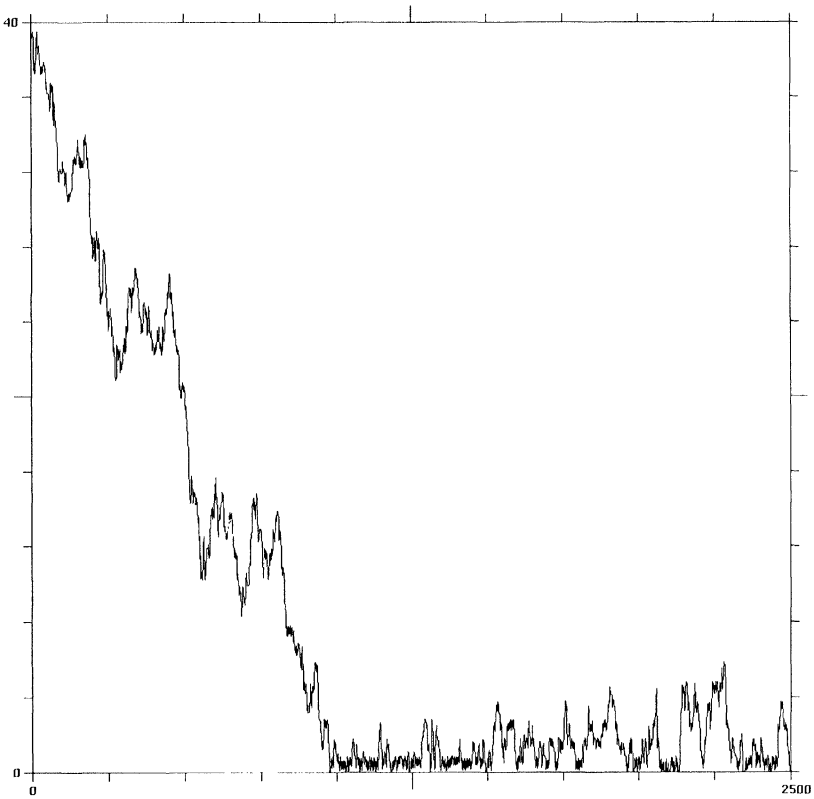


FIGURE 7 Time behavior of the first (x) variable of the staircase baker's map of Eq. (3). The numerical simulation starts out from a point in the antenna: Intial conditions: $x_0 = 39.9$, $y_0 = 0.0$. 2500 iterations.

antenna). With the resolution shown in Figure 6, the "basis" of the tower extends 500-fold to the right – to about 10 more meters to the right of this page, say. Thus, the present "tower" (if this word is an allowed description) is a rather broad and flat construction indeed.

The width of the antenna – the uppermost segment – is about one pixel in Figure 6. More precisely, we used 40 segments in the simulation, but only 20 of them are filled by any points at the simulation length presented. The antenna in the picture is the 20th segment. If the horizontal width is unity, the width of the antenna is 2^{-20}. that is, $10^{-6.3}$ (or, if the basis is 10 meters, about 3 micrometers).

One sees that the smooth "snow-like texture" of the "concrete" in Figure 5 has in Figure 6 (with its lesser resolution and longer simulation time) been turned into pitch-black. Thus, the property of volume conservation of the original baker's map is visibly heeded by a floating-point numerical calculation of Eq. (3).

5. FLARES IN THE STAIRCASE BAKER'S MAP

So far, we looked at both variables of Eq. (3) simultaneously that is, at the whole phase space. Next, we have a look at a single variable only,

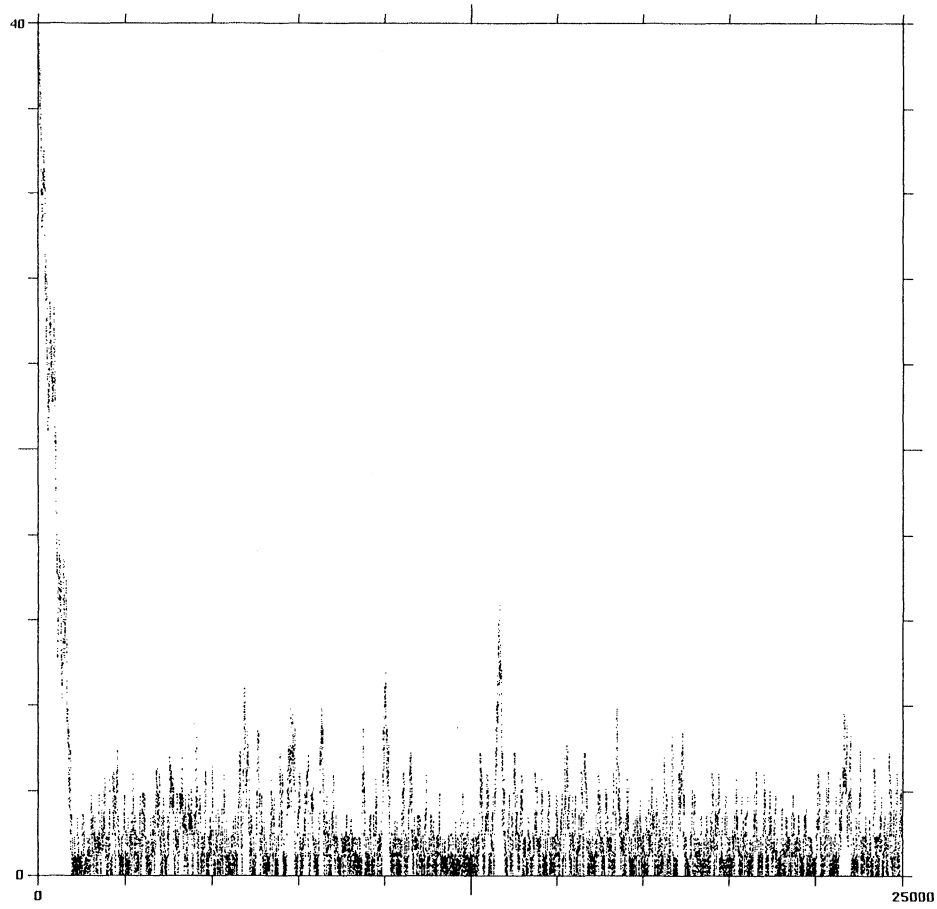


FIGURE 8 Ten times longer simulation than in Figure 7.

namely, at the time behavior of the vertical (x) variable in Figure 6.

Figure 7 shows a short piece of the time-behavior of the "height" of the state point (x variable) in the "tower" of Figure 6. The simulation starts out from an initial position in the antenna. One sees that height is very rapidly lost and that eventually, fluctuations around the "equilibrium" near the bottom occur. Qualitatively the same picture, but more "smoothly" (despite persitent peaks) will apply if the staircase is made smoother (10 percent rather ten 50 percent height per step).

Next, Figure 8 gives a ten-times longer rendering of the same time series. The next following picture, Figure 9, again gives a ten times longer simulation. One sees that eventually, at first lower, and after a while also higher, recapturings of more far-from-the-bottom initial positions occur. One thereby gets the impression that this example of a conservative two-dimensional map functions a bit analogously to the behavior of a multi-particle-gas (see Discussion).

We finish our presentation of numerical results with two much longer time series: Figures 10 and 11. While Figure 10 only continues the preceeding series, Figure 11 is different. The first part again shows a simulation of Eq. (3), but this time with the numerical code of Eq. (4) incorporated. Similar (but shorter in time) simulations were performed with up to 2^{18} binary digits (260 000 decimal digits accuracy). One has the impression that with sufficient accuracy and simulation length, eventually "recurrences" of up to fourty steps altitude will be achievable. Note that this would require 2^{40} iteration steps on average or some 10^{13} time steps.

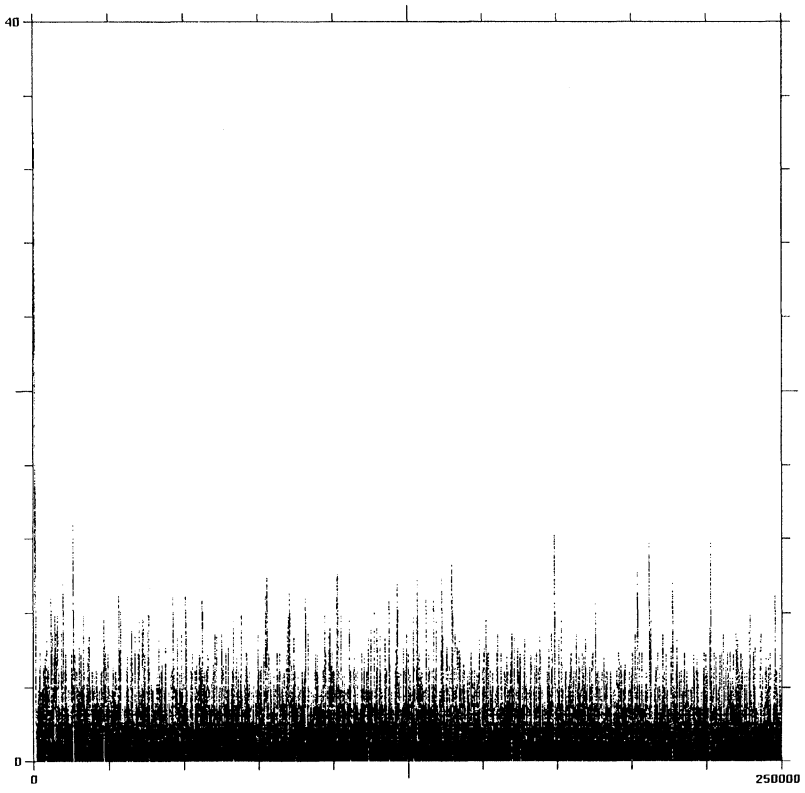


FIGURE 9 Ten times longer simulation than in Figure 8. 250 000 iterations.

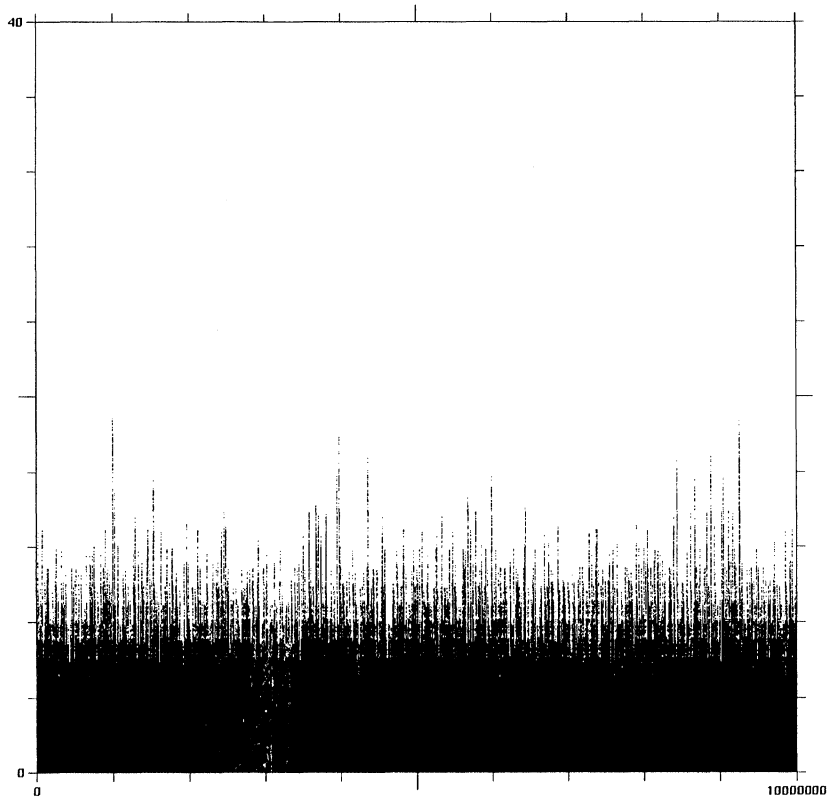


FIGURE 10 Forty times longer simulation than in Figure 9 (10 million iterations).

In the whole present series of pictures, from Figure 7 to Figure 11, first part (with its increased accuracy), one sees a field of "*Hopfenstangen*" (hop poles) as it were, with larger and larger poles interspersed as the simulation time is increased.

Figure 11, right-hand part, finally, is different. It represents a direct 100-times longer continuation of Figure 10. One sees a periodic recurrence.

In other words, if one continues the time series of Figure 7 on at double percision accuracy one finally ends up in a periodic regime, whose recurrence amplitudes are severely cut off. The same type of result is, by the way, also found with the potentially high-accuracy algorithm of Eq. (4) (if the accuracy has comparably low value). Each time, a different "periodic recurrence" is found.

6. ON THE HISTORY OF MULTI-BAKER'S MAPS

The invention of the map, which is today called a 'multi-baker's map', is due to Eberhard Hopf, as mentioned. He not only introduced a semi-infinite baker's map, but also proved mixing for this dynamical system. Further ergodic properties of the bi-infinite chain of baker's maps were proved by Goldstein and Leibowitz [11] in 1974 in connection with investigations of the Lorentz gas. Renewed interest was triggered by the work of Gaspard [12] and the observation of fractal eigenstates by Hasegawa [13] and Tasaki [14]. Later, inhomogeneous versions of baker's maps (where the cell size varies as a function of the extended coordinate) were apparently first considered

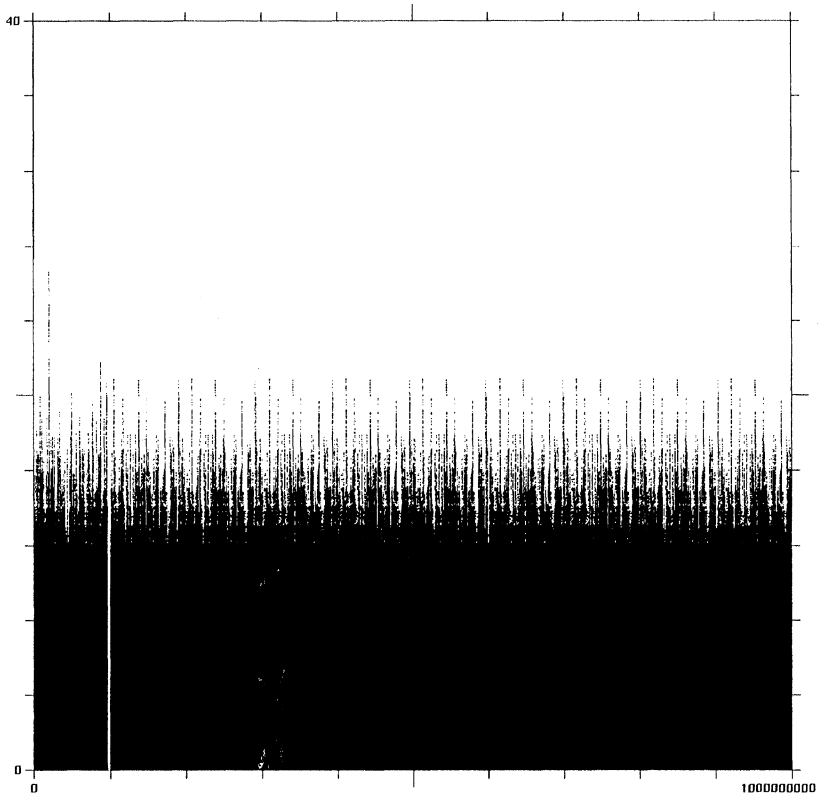


FIGURE 11 A hundred times longer calculation then in Figure 10, in two potions. The first portion occupies the first ten percent of the picture and contains 100 million timesteps, ten times more than Figure 10. The second, longer portion has the same resulation and hence is an hundred times longer version of Figure 10. One sees on closer inspection that a periodically recurring pattern has set in, with a period of about 100 million time steps. The series of pictures beginning with Figure 7 thus ends up in periodicy. The first portion here, in contrast, was calculated at 8192 binary digits accuracy (corresponding to 2600 decimal digits), using the algorhithm of Eq. (4). Note the single, much higher peak there.

in [15, 16] in connection with disordered chaotic maps [17], and independently in [18] for exponentially decaying cell sizes.

7. DISCUSSION

We have presented a very simple 2D map and looked at it numerically. The map is "mixing" in the sense of Hopf [9]—chaotic with an equal density everywhere. The qualitative behavior is just as it was expected to be: very rarely, a pre-assigned, very thin region is visited (the "antenna"). An exponential distribution is thereby generated as far as height is concerned, $P = 2^{-x}$. More exactly, the cell-to-cell dynamics can be mimicked as a one-dimensional discrete random walk with partially reflecting boundary conditions and otherwise spatially constant transition probabilities. Such models were studied in depth by Mark Kac [19] (and more recently within the thermodynamic formalism in [20]). The connection with random walks, as presented, *e.g.*, in [16], implies that the first return times for this model can be calculated exactly with the methods of [19]. This connection also explains why the mean times of first return increase much slower with the distance from the origin here, than is the case in urn models (which were also treated in [19]). Basically this reflects the differences between

Brownian motions in triangular respectively parabolic potentials.

Thus, statistically speaking, everything appears trivial in a sense. Nevertheless, the present system has an interest not only from as statistical point of view. This is because the "flaring behavior" interpretation gives one a new "feel" for the deterministic Boltzmann-type dynamics that is at work here.

Recently, a continuous molecular-dynamics simulation of a Boltzmann gas of repulsive particles in two dimensions for the first time allowed the description of a "deterministic entropy" based on the momentarily occupied phase-space volume [21]. This finding triggered the present investigation into a hypothetically analogous deterministic system of discrete type. The existence of a connection between the baker's transformation on the one hand and continuous billiard systems of the Sinai type on the other is, of course, a well-known fact in its own right (see, *e.g.* [22]).

It appears to us that the qualitatitve insights first gained by Boltzmann with his famous H function and recently confirmed in the above mentioned molecular-dynamics simulation by means of an "improved H-function" [21], are in qualitative agreement with the "flaring-type interpretation" of the present system. While many "Poincaré cycles" cannot usually be inspected in a gas since the recurrence times are forbidding even for small particle numbers as is well known, with the present simple analogue, such cycles can be studied numerically for the first time in a determinisitc reversible system. Note that this is what Figures 7–11 really show. Never before to our knowledge have Poincaré cycles been observed explicitly as a far-from-equilibrium deterministic phenomenon.

At this point the connection between the present baker's map and the random multibaker's map [15] deserves to be discussed. We do this best in a stepwise manner. Note that in the present baker's map, nothing prevents us from using two (or more) antennas instead of one. Flares of different identities ("colors") could then be observed in our system. The idea that a physical system that approaches equilibrium may still bear the "birthmarks" of several alternative, far-from-equilibrium initial states ("flares" of different colours) is somewhat counterintuitive at first sight and appears to be new. Nevertheless the number of peaks can (a) be increased and (b) be "rearranged". Indeed the whole ordered map can be rearranged in a disorderly fashion. This limiting other extremal case was described in [17] as an example of a system which shows "localization" in a transport process. The consequence was an unexpected "trapping" of the state point in midvoyage for exponentially long waiting times. The transition between the present "idealized" version (which was found independently [18] as mentioned) and the "disorded" alternative appears to be highly nontrivial: Does there exist a short bifurcation separating multi-colour Poincaré recurrences from "glassy" localization?

At last, we turn to the numerical finding in the right-hand part of Figure 11. Tom Rogers [23] in 1981 described the existence of numerically generated periodic cycles in one-dimensional maps as a function of bin size, that is, as a function of digital accuracy. A similar phenomenon has now been found in numerical calculations of the present reversible discrete chaotic and potentially far-from-equilibrium systems. While it is not surprising that manifest periodic cycles are generated as numerical artifacts, it is somewhat unexpected that so extremely long recurrences are generated in the presence of moderate bin size. This numerical finding is perhaps not very important. Nevertheless it suggests the following conclusion when a translation back into nature is attempted : Very far-from-equilibrium initial conditions cannot be realized spontaneously in reversible systems by nature unless the accuracy of its calculations is very high indeed. Thus, if nature belongs into the ballpark of reversible systems, as Boltzmann thought, its accuracy of calculation must be awe-inspiring. This result possibly carries over to quantum mechanics (Hans Primas, personal communication).

To conclude, a simple map of a possibly new type has been presented and investigated numerically. The behavior of deterministic, far-from-equilibrium continuous Hamiltonian systems, studied previously, could thereby be mimicked in a qualitative fashion it appears. The behavior of staircase baker's maps is a "toy model" for the study of Poincaré recurrences in reversible systems.

Acknowledgments

Invited paper presented, under the title "Flares as *H*-function peaks in multi-baker's map", at the First International Conference on Discrete Chaotic Dynamics in Nature and Society (DCDNS), Beer-Sheva, October 19–22, 1998. O. E. R. acknowledges travel support by the DFG. We thank Vladimir Gontar, Michael Sonis, Peter Plath, Gustaf Kristiansen, Benoit Mandelbrot, Ilja Prigogine, Norman Packard, S. Tasaki, Pierre Gaspard, John Antoniu, Grégoire Nicolis, Dietrich Hoffmann, Daniel Neumann, Dieter Fröhlich, Gerold Baier, Larry Horwitz and Barkley Rosser for stimulating discussions. For J.O.R.

References

[1] Hartmann, G. C. and Rössler, O. E. (1998). Coupled flare attractores. *Discrete Dynamics in Nature and Society*, **2**, 153–159.
[2] Rosser, B., *Volatility via social flaring*. James Madison University, Harrisburg, http://cob.jmu.edu/rosserjb/VOLATILE.FLR.doc, February, 1999.
[3] Jahn, F., *A life for Wienerwald: From Waiter to Millionaire and Back* (*in German*). Wienerwald Publ., Munich, 1993.
[4] Rossler, O. E. and Hartmann, G. C. (1995). Attractors with flares. *Fractals*, **3**(2), 285–296.
[5] Milnor, J. (1985). On the concept of attractor. *Commun. Math. Phys.*, **99**, 177–195.
[6] Tsuda, I. and Nicolis, G., Preprint, 1999.
[7] von Weizsäcker, C. F. (1939). *Annalen der Physik*, **36**, 275.
[8] Boltzmann, L., *Lectures on Gas Theory*. John Ambrosius Barth, Leipzig, 1898.
[9] Hopf, E., *Ergodentheorie*. Springer Verlag, Berlin, 1937.
[10] Argyris, J., Faust, G. and Haase, M., *Die Erforschung des Chaos*. Vieweg, Wiesbaden, 1995.
[11] Goldstein, S. and Lebowitz, J. L. (1974). Ergodic properties of an infinite system of particles moving independently in a periodic field. *Comm. Math. Phys.*, **37**, 1–18.
[12] Gaspard, P. (1992). Diffusion, effusion and chaotic scattering: An exactly solvable liouvillian dynamics. *J. Stat. Phys.*, **68**, 673–747.
[13] Hasegawa, H. H. and Driebe, D. J. (1994). Intrinsic irreversibility and the validity of the kinetic description of chaotic systems. *Phys. Rev. E*, **50**(3), 1781–1809.
[14] Tasaki, S. and Gaspard, P. (1995) Fick's law and fractality of nonequilibrium stationary states in a reversible multi-baker map. *J. Stat. Phys.*, **81**, 935–987.
[15] Radons, G., Talk presented at the workshop on "Stochasticity and Structure Formation", Behn, U., Kühnel, A. and Schiele, K. (orgs.), Leipzig, 1996; and talk presented at the workshop on "Hyperbolic Systems with Singularities", Szasz, D. and Choquard, P. (orgs.), Erwin-Schrödinger-Institut. Wien, 1996.
[16] Radons, G. (1999). Disorder phenomena in chaotic systems. *Festkörperprobleme*, *Advances in Solid State Physics*, **38**, 439–451.
[17] Radons, G. (1996). Suppression of chaotic diffusion by quenched disorder. *Phys. Rev. Lett.*, **77**, 4748–4751.
[18] Rössler, O. E. and Hartmann, G. C., *Talk presented at the Workshop on "Disorded Dynamical Systems"*, Radons, G. (org.). Dresden, 1998.
[19] Kac, M. (1947). Random walk and the theory of brownian motion. *Am. Math. Month.*, **54**(7), 369–391.
[20] Radons, G. (1995). Thermodynamic analysis of inhomogeneous random walks: Localization and phase transitions. *Phys. Rev. Lett.*, **75**, 4719–4723.
[21] Diebner, H. H. and Rössler, O. E. (1998) A deterministic entropy based on the instantaneous phase space volume. *Z. Naturforsch.*, **53a**, 51–60.
[22] Vollmer, J. (1996). *On Pruned Baker's Map and Transient Chaos. Ph. D. Thesis*, Faculty of Philosophicy and Natural Sciences, University of Basel.
[23] Rogers, T., In: Rosen, R. Ed., *Progress in theoretical biology*. Academic Press, New York, 1981.

Journal of Applied Mathematics and Decision Sciences

Special Issue on
Intelligent Computational Methods for Financial Engineering

Call for Papers

As a multidisciplinary field, financial engineering is becoming increasingly important in today's economic and financial world, especially in areas such as portfolio management, asset valuation and prediction, fraud detection, and credit risk management. For example, in a credit risk context, the recently approved Basel II guidelines advise financial institutions to build comprehensible credit risk models in order to optimize their capital allocation policy. Computational methods are being intensively studied and applied to improve the quality of the financial decisions that need to be made. Until now, computational methods and models are central to the analysis of economic and financial decisions.

However, more and more researchers have found that the financial environment is not ruled by mathematical distributions or statistical models. In such situations, some attempts have also been made to develop financial engineering models using intelligent computing approaches. For example, an artificial neural network (ANN) is a nonparametric estimation technique which does not make any distributional assumptions regarding the underlying asset. Instead, ANN approach develops a model using sets of unknown parameters and lets the optimization routine seek the best fitting parameters to obtain the desired results. The main aim of this special issue is not to merely illustrate the superior performance of a new intelligent computational method, but also to demonstrate how it can be used effectively in a financial engineering environment to improve and facilitate financial decision making. In this sense, the submissions should especially address how the results of estimated computational models (e.g., ANN, support vector machines, evolutionary algorithm, and fuzzy models) can be used to develop intelligent, easy-to-use, and/or comprehensible computational systems (e.g., decision support systems, agent-based system, and web-based systems)

This special issue will include (but not be limited to) the following topics:

- **Computational methods**: artificial intelligence, neural networks, evolutionary algorithms, fuzzy inference, hybrid learning, ensemble learning, cooperative learning, multiagent learning
- **Application fields**: asset valuation and prediction, asset allocation and portfolio selection, bankruptcy prediction, fraud detection, credit risk management
- **Implementation aspects**: decision support systems, expert systems, information systems, intelligent agents, web service, monitoring, deployment, implementation

Authors should follow the Journal of Applied Mathematics and Decision Sciences manuscript format described at the journal site http://www.hindawi.com/journals/jamds/. Prospective authors should submit an electronic copy of their complete manuscript through the journal Manuscript Tracking System at http://mts.hindawi.com/, according to the following timetable:

Manuscript Due	December 1, 2008
First Round of Reviews	March 1, 2009
Publication Date	June 1, 2009

Guest Editors

Lean Yu, Academy of Mathematics and Systems Science, Chinese Academy of Sciences, Beijing 100190, China; Department of Management Sciences, City University of Hong Kong, Tat Chee Avenue, Kowloon, Hong Kong; yulean@amss.ac.cn

Shouyang Wang, Academy of Mathematics and Systems Science, Chinese Academy of Sciences, Beijing 100190, China; sywang@amss.ac.cn

K. K. Lai, Department of Management Sciences, City University of Hong Kong, Tat Chee Avenue, Kowloon, Hong Kong; mskklai@cityu.edu.hk